Original Article

Poly(ADP-Ribose) Polymerase Inhibitors Ameliorate Nephropathy of Type 2 Diabetic Lepr$^{db/db}$ Mice

Csaba Szabó,[1] Alisha Biser,[2] Rita Benkő,[3] Erwin Böttinger,[4] and Katalin Suszták[2]

The activation of the poly(ADP-ribose) polymerase (PARP) plays an important role in the pathophysiology of various diseases associated with oxidative stress. We found increased amounts of poly(ADP) ribosylated proteins in diabetic kidneys of Lepr$^{db/db}$ (BKsJ) mice, suggesting increased PARP activity. Therefore, we examined the effects of two structurally unrelated PARP inhibitors (INO-1001 and PJ-34) on the development of diabetic nephropathy of Lepr$^{db/db}$ (BKsJ) mice, an experimental model of type 2 diabetes. INO-1001 and PJ-34 were administered in the drinking water to Lepr$^{db/db}$ mice. Both INO-1001 and PJ-34 treatment ameliorated diabetes-induced albumin excretion and mesangial expansion, which are hallmarks of diabetic nephropathy. PARP inhibitors decreased diabetes-induced podocyte depletion in vivo and blocked hyperglycemia-induced podocyte apoptosis in vitro. High glucose treatment of podocytes in vitro led to an early increase of poly(ADP) ribosylated modified protein levels. Reactive oxygen species (ROS) generation appears to be a downstream target of hyperglycemia-induced PARP activation, as PARP inhibitors blocked the hyperglycemia-induced ROS generation in podocytes. INO-1001 and PJ-34 also normalized the hyperglycemia-induced mitochondrial depolarization. PARP blockade by INO-1001 and PJ-34 prevented hyperglycemia-induced nuclear factor-κB (NFκB) activation of podocytes, and it was made evident by the inhibitor of κBα phosphorylation and NFκB p50 nuclear translocation. Our results indicate that hyperglycemia-induced PARP activation plays an important role in the pathogenesis of glomerulopathy associated with type 2 diabetes and could serve as a novel therapeutic target.
***Diabetes* 55:3004–3012, 2006**

Diabetic nephropathy is the leading cause of end-stage renal disease in the U.S. (1). Characteristic morphological lesions of diabetic nephropathy initially present in the renal glomerulus; these include glomerular hypertrophy, thickening of the basement membrane, and mesangial expansion (2). Several interventions have been shown to slow the progression of diabetic nephropathy, including tight glucose and blood pressure control and the blockade of the renin-angiotensin system (3–5). However, none of these can cure or prevent the development of diabetic nephropathy.

Recent observations indicate important roles for glomerular epithelial cells (podocytes) in the pathogenesis of diabetic nephropathy (6–9). The density of glomerular visceral epithelial cells is reduced in kidneys of individuals with diabetic nephropathy. Among various glomerular morphological characteristics, the decreased podocyte density is one of the strongest predictors of disease progression (10). Apoptosis and detachment of podocytes have been implicated as a potential mechanism of podocyte loss in animal models of diabetic nephropathy (7,11). We recently reported increased apoptosis of podocytes in type 1 diabetic Akita and type 2 diabetic Lepr$^{db/db}$ mice at the time of development of hyperglycemia. In vitro treatment of podocytes with high glucose also leads to increased apoptosis rate (7,12). Podocyte apoptosis seems to contribute significantly to the development of diabetic nephropathy, as prevention of podocyte apoptosis in vivo was associated with a decrease in albuminuria and mesangial expansion in the Lepr$^{db/db}$ model of type 2 diabetes.

Brownlee (13) has pioneered the concept that hyperglycemia-induced overproduction of superoxide is the single unifying link to diabetes complications, including cellular activation of protein kinase C, hexosamine pathway, and advanced glycation formation, which are the major pathways of hyperglycemic damage in endothelial cells. This process occurs via inhibition of glyceraldehyde-3-phosphate dehydrogenase activity, which is likely to be the consequence of poly(ADP) ribosylation of the enzyme by active poly(ADP-ribose) polymerase (PARP)-1 (14). Since uncoupling protein 1 or manganese superoxide dismutase overexpressions blocked the activation of PARP-1, it has been hypothesized that the high-glucose–induced PARP-1 activation is the consequence of the increased intracellular reactive oxygen species (ROS) and subsequent DNA breakage in endothelial cells (14).

PARP-1 is one of the most abundant nuclear proteins. The catalytic function of PARP-1 relates to its role as a DNA damage sensor and signaling molecule. The zinc

From the [1]Department of Surgery, University of Medicine and Dentistry of New Jersey, Newark, New Jersey; the [2]Division of Nephrology, Department of Medicine, Albert Einstein College of Medicine, Bronx, New York; the [3]Department of Human Physiology and Clinical Experimental Research, Semmelweis University Medical School, Budapest, Hungary; and the [4]Department of Medicine, Mount Sinai School of Medicine, New York, New York.

Address correspondence and reprint requests to Katalin Susztak, Division of Nephrology, Albert Einstein College of Medicine, Bronx, NY 10461. E-mail: ksusztak@aecom.yu.edu.

Received for publication 1 February 2006 and accepted in revised form 1 August 2006.

C.S. is a stockholder of Inotek Pharmaceuticals, a firm involved in the development of PARP inhibitors.

Additional information for this article can be found in an online appendix at http://diabetes.diabetesjournals.org.

ELISA, enzyme-linked immunosorbent assay; IκBα, inhibitor of κBα; NFκB; nuclear factor-κB; PARP, poly(ADP-ribose) polymerase; PAS, periodic acid Schiff; ROS, reactive oxygen species.

DOI: 10.2337/db06-0147

fingers of PARP recognize single- and double-stranded DNA breaks. PARP-1 subsequently forms heterodimers and catalyzes the cleveage of NAD^+ into nicotinamide and ADP-ribose; the latter is used to synthesize branched nucleic acid–like polymers that are covalently attached to acceptor proteins (15). Most of the biological effects of PARP relate to the various aspects of this process: *1*) covalent poly(ADP) ribosylation, which influences function of target proteins; *2*) poly(ADP) ribosylated oligomers that, when cleaved from poly(ADP) ribosylated proteins, confer distinct cellular effects; *3*) the physical association of PARP with other nuclear proteins; *4*) the lowering of the cellular level of NAD^+ (its substrate); and *5*) DNA repair (15).

During the past decade, structure-based drug design and increased understanding of molecular details of active PARP-1 facilitated the discovery of highly potent PARP inhibitors. Inhibitors can be divided into two basic categories: *1*) nucleic acid and nucleoside derivatives and *2*) structure-based inhibitors that bind to the PARP catalytic fragment, including highly potent (orally available) inhibitors like PJ-34 and INO-1001, developed by Inotek Pharmaceuticals (with half-maximal inhibitory concentration of 1 nmol/l for INO-1001) (16). Some of these compounds, including the INO-1001, are in phase I and II. Clinical trials for myocardial infarction and for other indications appear to be well tolerated clinically (17).

Studies based on the use of various PARP inhibitors and genetic ablation of PARP-1 (PARP-1 knockout mice) indicate that PARP plays an important role in the development of multiple disease conditions including stroke, myocardial infarction, heart failure, vascular dysfunction, and mesenteric, muscle, or renal ischemia reperfusion injury, among others (18–20). PARP has also been suggested to play a role in the development of type 1 diabetes. PARP-1 knockout mice are protected from the development of streptozotocin-induced diabetes (21). In addition, PARP might also contribute to complications of type 1 diabetes. PARP inhibitors ameliorate endothelial and myocardial dysfunction, peripheral and autonomic neuropathy, and retinopathy of streptozotocin-induced mouse or rat diabetic models (14,22–25). Recent studies by Minchenko et al. (26) found increased PARP activity in the renal tubuli of streptozotocin-induced diabetic rats 2 weeks after a single-dose streptozotocin injection. However, structural tubular damage (i.e., atrophy and tubulointerstitial fibrosis) does not occur until late in diabetic nephropathy (27,28).

Clinical studies suggest altered activity of PARP-1 in monocytes of type 2 diabetic patients and an increased expression of PARP-1 in skin biopsies of patients with type 2 diabetes (29). The functional role of PARP in diabetic nephropathy and in type 2 diabetes has not yet been investigated. Here, we used two different highly potent PARP inhibitors to examine the role of the PARP pathway in nephropathy, which is characteristic of type 2 diabetic mice. We report that PARP inhibition attenuates the development of both diabetic mesangial expansion and albuminuria. We hypothesized that the inhibition of ROS generation, normalization of mitochondrial function, and nuclear factor-κB (NFκB) activation is the likely mode of PARP inhibitors' protective action.

RESEARCH DESIGN AND METHODS

Reagents. PJ-34 and INO-1001 were synthesized at Inotek Pharmaceuticals (Beverly, MA). PJ-34 was purchased from Alexis Biochemicals (Axxora, San Diego, CA).

Animals and experimental protocols. Male *db/db* ($Lepr^{db/db}$) mice, together with nondiabetic control *db/m* mice on C57BLKs/J background (Jackson Laboratories, Bar Harbor, ME), were used. INO-1001 and PJ-34 treatment were initiated at 5 weeks of age. In sterile water that was sweetened with NutraSweet, 4.8 g/l INO-1001 and 2.4 g/l PJ-34 was dissolved. Control animals received sweetened water only. The average inhibitor consumption was 60 mg/kg INO-1001 and 30 mg/kg PJ-34. All animal protocols and procedures were approved by the institutional animal care and use committee at the Albert Einstein College of Medicine and at the Mount Sinai School of Medicine.

For determination of urinary albumin excretion, mice were placed in individual metabolic cages (Nalgene Nunc, Rochester, NY) and urine collected for 16 h. Urinary albumin was measured using an enzyme-linked immunosorbent assay (ELISA) specific for mouse albumin (Albuwell; Exocell, Philadelphia, PA), and urine creatinine was determined using Creatinine Companion (Exocell). Blood glucose was measured with Glucometer Elite (Bayer) after 6 h of fasting. Animals were killed at 17–21 weeks of age, when significant albuminuria and mesangial expansion occurs.

Renal histology and immunohistochemistry. For analysis of glomerular histology, formalin-fixed, paraffin-embedded kidney tissue sections were stained with periodic acid Schiff (PAS) reagent and coded and read by an investigator who was unaware of the experimental protocol. Mesangial matrix expansion was evaluated semiquantitatively on 50 glomeruli per kidney, using a score of 1 for minimal, 2 for mild mesangial matrix expansion, 3 for moderate, and 4 for diffuse mesangial matrix expansion.

Podocyte number per glomerular cross section was determined on 4-μm frozen sections double stained with WT-1 (rabbit) (Santa Cruz Biotechnology, Santa Cruz, CA) and synaptopodin (mouse) as described earlier (30) and developed with fluorescein isothiocyanate–conjugated anti-mouse and Cy3-conjugated anti-rabbit secondary antibodies (Jackson Immunologicals). Only cells stained positive for both synaptopodin and WT-1 were counted. NFκB p50 and synaptopodin double immunostaining was performed similarly using NFκB p50 (rabbit) (Santa Cruz Biotechnology) and anti synaptopodin (mouse) antibodies.

Poly(ADP) ribosylated staining was performed using mouse anti–poly-(ADP)-ribose (Alexis) antibody. Briefly, after deparaffinization, the tissue was treated in 10 mmol/l sodium citrate and microwaved. After blocking, sections were incubated with the primary antibody 1:50 dilution overnight at 4°C. Signal was developed using ABC Vectastain Elite kit (Vector Laboratories, Burlington, CA).

Western blot analysis. Whole-kidney samples were homogenized in radioimmunoprecipitation assay buffer. Proteins were separated on 10% SDS gels and transferred to polyvinylidine fluoride membranes. Blots were incubated using mouse anti–poly(ADP)-ribose antibody (1:1,000 dilution), followed by peroxidase-conjugated goat anti-mouse antibody and developed with ECL chemiluminescence kit (Pierce). Blots were reprobed with mouse anti-αtubulin antibody (Sigma Aldrich) as a loading control. Western blot analyses on podocyte lysates were performed similarly by using anti-PAR (Alexis), phospho-IκBα (inhibitor of κBα; Santa Cruz Biotechnology), and tubulin (Sigma) antibodies.

Cell culture. Cultivation of conditionally immortalized mouse podocytes was performed as described (31). Briefly, cells were propagated in the undifferentiated state on type 1 collagen at 33°C in RPMI-1640 in the presence of 10% fetal bovine serum (Hyclone) and 20 units/ml interferon-γ (Sigma Chemical, St. Louis, MO). To induce differentiation, cells were maintained at 37°C without interferon for 10 days. All experiments were performed using differentiated podocytes. Before the experiment, cells were incubated overnight in RPMI with 0.2% fetal bovine serum containing 5 mmol/l glucose.

Apoptosis detection. Apoptotic nuclei of cultured podocytes were detected on paraformaldehyde-fixed cells using DAPI (4′,6-diamidino-2-phenylindole) staining (1 μg/ml) for 10 min. Cells were analyzed under a fluorescence microscope and assessed for chromatin condensation and segregation. Caspase-3 activity was measured in podocyte extracts using EnzCheck Caspase-3 Assay kit (Molecular Probes) following the manufacturer's protocol.

Nuclear extracts were prepared using Transfactor DB Nuclear extraction kit (Clontech BD Bioscience) following the manufacturer's protocol. Western blotting was performed using NFκB p50 (Santa Cruz Biotechnology) antibody. NFκB p50 nuclear binding assay was performed using TransFactor Colorimetric kit (Clontech BD) according to the manufacturer's protocol.

Determination of ROS generation. For kinetic studies, podocytes were plated on 24-well plates, loaded with 50 μmol/l carboxymethyl-H_2-dichlorofluorescein diacetate (CM-H_2DCFDA; Invitrogen) for 30 min at 37°C, washed twice with PBS, and incubated with PJ-34 (3 μmol/l) or INO-1001 (200 nmol/l) for 30 min, followed by stimulation with 30 mmol/l D-glucose or 30 mmol/l L-glucose. Fluorescence was analyzed using Wallac Victor^2 Fluorescence Plate Reader (7).

Determination of mitochondrial membrane potential. Podocytes, grown on coverslips, were loaded with 1 μg/ml JC-1 (Invitrogen) for 20 min at 37°C. Coverslips were rinsed with PBS five times, and cells were maintained at 37°C and either left untreated or pretreated with INO-1001 (200 nmol/l) or PJ-34 (3 μmol/l) for 30 min, followed by incubation in 5 or 30 mmol/l D-glucose. To view J-aggregates, excitation and emission were recorded with a charged-coupled device camera at 543–560 nm and at 480–530 nm for monomeric. For each coverslip, five images of each condition were analyzed (32). Flow cytometry cells were incubated in 5 or 30 mmol/l D-glucose in the presence or absence of the inhibitors, trypsinized, loaded with 5 μg/ml JC-1, and washed twice with PBS, and 10,000 cells/condition were analyzed with FACScan (AECOM Shared Scientific Facilities).

Statistical analysis. All results are expressed as means ± SE. The data were analyzed by Student's *t* test. Differences were considered statistically significant when the *P* values were <0.05.

RESULTS

Changes in blood glucose and body weight in control and inhibitor-treated mice. We evaluated the effect of two structurally unrelated PARP inhibitors, PJ-34 and INO-1001, on the development of diabetic nephropathy of Lepr$^{db/db}$ mice. The Lepr$^{db/db}$ mice suffer from obesity and develop diabetes around 8 weeks of age (33,34). PARP inhibitors were administered in the drinking water, starting at 5 weeks of age. Blood levels of INO-1001 were also determined in serum samples using high-performance liquid chromatography method, and it ranged between 46 and 109 nmol/l. Treatment with the PARP inhibitors did not cause any excess mortality or any obvious phenotype change in diabetic and control mice; there was no significant difference in the body weight of control and inhibitor-treated *db/db* mice (Table 1). Neither PJ-34 nor INO-1001 inhibited the development of diabetes in this type 2 diabetes model (defined as fasting blood glucose >250 mg/dl). However, PJ-34–treated mice had lower serum glucose values than control *db/db* animals (501 ± 19 vs. 595 ± 2.5 mg/dl, respectively) (Table 1). There was no statistical difference in the serum glucose values in the control and INO-1001–treated *db/db* mice. In summary, oral administration of both inhibitors were well tolerated by the animals.

TABLE 1
Body weight and serum glucose levels of control, PJ-34–, or INO-1001–treated diabetic Lepr$^{db/db}$ (BKLsJ) and nondiabetic Lepr$^{db/db}$ mice

Group	*n*	Age (weeks)	Body weight (g)	Blood glucose (mg/dl)
*db/m*CTL	10	21	28 ± 0.5	126 ± 5.5
db/m INO	10	21	25.9 ± 1.5	148 ± 10.3
db/db CTL	10	21	43.8 ± 1.1	600 ± 1
db/db INO	10	21	47.1 ± 1.6	562 ± 19
db/m CTL	8	17	28 ± 1.6	133 ± 6.2
db/db CTL	8	17	46.3 ± 2	595 ± 2.5
db/db PJ-34	8	17	47.1 ± 1.6	501 ± 19*

Data are means ± SE unless otherwise indicated. *$P < 0.05$. CTL, control; INO, INO-1001.

Diabetes induces PARP activation in the kidney. Increased PARP activity has been described in various tissues in diabetes. Using an antibody that specifically detects poly(ADP) ribosylated proteins, products of the active enzyme, various poly(ADRP) ribosylated proteins can be visualized as multiple bands on Western blots. We found a marked increase in the amount of poly(ADP) ribosylated proteins in renal extracts of 17- and 21-week-old diabetic (*db/db* control) mice compared with nondiabetic *db/m* mice (Fig. 1*A*). Diabetic mice treated with the PARP inhibitors had lower amount of poly(ADP) ribosylated proteins in kidney extracts compared with untreated diabetic mice. Quantification/densitometry of the poly-(ADP) ribosylated proteins compared with the loading control tubulin is shown in Fig. 1*B*. To determine in which cell type PARP is activated, we performed immunostaining with an anti–poly(ADP) ribosylated antibody in kidney sections of control (*db/m*), diabetic *db/db*, and *db/db* mice

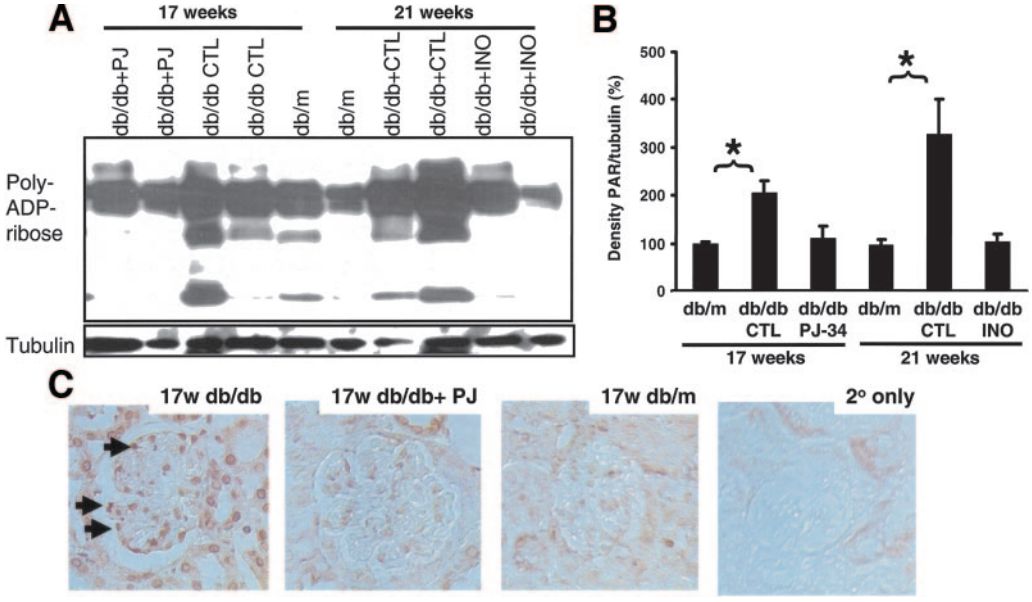

FIG. 1. Increased poly(ADP) ribosylated protein content in diabetic *db/db* mice compared with nondiabetic mice (*A*). Western blot analysis with anti–poly(ADP) ribosylated antibody of whole-kidney lysates of 21- or 17-week-old control (CTL) diabetic *db/db* and PJ-34– or INO-1001–treated *db/db* diabetic or nondiabetic *db/m* kidneys. *B*: Average relative density of all poly(ADP) ribosylated–modified proteins in relation to αtubulin. The data were normalized (100%) to 17-week-old *db/m* mice (*C*). Representative immunostaining of kidney sections of 17-week-old control *db/db*, PJ-34–treated *db/db*, and nondiabetic *db/m* mice. Slides were stained with (or without) anti–poly(ADP) ribosylated antibody and developed with peroxidase-conjugated secondary antibody (without counterstaining). Arrows indicate positive podocyte staining.

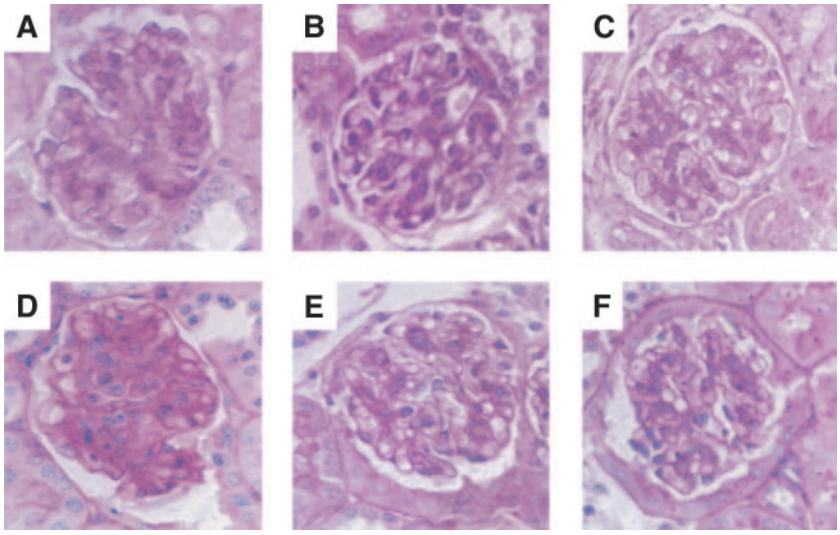

FIG. 2. Representative photographs of PAS-stained kidney sections from 17-week-old control *db/db* animals (*A*), 17-week-old PJ-34–treated *db/db* animals (*B*), 17-week-old control *db/m* mice (*C*), 21-week-old control *db/db* animals (*D*), 21-week-old INO-1001–treated *db/db* animals (*E*), and 21-week-old control *db/m* mice (*F*).

treated with PJ-34. There was an overall increase in the amount of poly(ADP) ribosylated–modified proteins in kidneys of diabetic mice. As shown in Fig. 1*C*, poly(ADP) ribosylated–modified proteins were also increased in glomerular podocytes of diabetic mice (Fig. 1*C*). This increase was already evident at 8 weeks of age (online appendix Fig. 1 [available at http://diabetes.diabetesjournals.org]) at the time of development of diabetes. PJ-34– and INO-1001–treated animals had lower glomerular poly(ADP) ribosylated staining; however, some tubular cells remained positive. In summary, we found increased PARP activity in the diabetic kidneys, particularly in podocytes.

PARP inhibition ameliorates the development of diabetic nephropathy in *db/db* mice. Next, we examined the development of diabetic nephropathy in control and PARP inhibitor–treated *db/db* mice. As shown in Fig. 2, diabetic *db/db* mice treated with INO-1001 or PJ-34 had significantly less mesangial expansion than control *db/db* mice. Semiquantitative analysis of PAS-stained kidney sections showed that 21-week-old diabetic mice treated with INO-1001 had a mesangial expansion score (on a scale of 1–4) of 2.3 ± 0.4 vs. 3.6 ± 0.2 of control *db/db* mice (Table 2). Similarly, 17-week-old diabetic mice treated with PJ-34 also had significantly less glomerular disease than untreated diabetic mice (1.4 ± 0.3 vs. 2.9 ± 0.3 arbitrary units). Albuminuria, a hallmark of diabetic renal disease, was also decreased in mice treated with PARP inhibitors. As quantitated by mouse albumin-specific ELISA, control *db/db* mice had 1,036 ± 180 μg/mg (albumin/creatinine) albuminuria compared with mice treated with INO-1001, which had only 440 ± 71 μg/mg (albumin/creatinine) albuminuria (>50% reduction). A similar reduction was observed following PJ-34 treatment (Table 2). In summary, both inhibitors ameliorated diabetic mesangial expansion and albuminuria, the two hallmarks of diabetic nephropathy in the *db/db* model of type 2 diabetes.

PJ-34 and INO-1001 prevent podocyte depletion. Since depletion of glomerular podocytes correlates with albuminuria and disease progression in diabetic nephropathy (7,35), we next evaluated podocyte number in control and inhibitor-treated diabetic mice. Diabetic *db/db* mice have significantly lower podocyte number per glomerular profile than age-matched control *db/m* mice; their numbers amounted at 7.5 ± 1 in 17-week-old *db/db* mice vs. 10.2 ± 0.4 in *db/m* animals (Table 2). Diabetic mice treated with PJ-34 had an average of 9.6 ± 1.4 podocyte number per glomerular profile, which was statistically different from untreated *db/db* mice. Similar results were obtained with INO-1001 treatment (Table 2). Thus, both PARP inhibitors prevented podocyte depletion in diabetic animal models.

Hyperglycemia induces PARP activation of cultured podocytes. Next, we determined whether high glucose leads to PARP activation in vitro by using cultured murine podocytes. We found increased levels of poly(ADP) ribosylated–modified proteins in podocytes as early as 60 min after incubation in 30 mmol/l D-glucose (Fig. 3). Both INO-1001 and PJ-34 significantly decreased the amount of poly(ADP) ribosylated–modified proteins. In summary, we found increased poly(ADP) ribosylated–modified proteins, likely indicating increased PARP activity, in podocytes following incubation in hyperglycemic milieu.

TABLE 2
Effect of PARP inhibition on the development of diabetic nephropathy in *db/db* mice

Group	Albumin/creatinine (μg/mg)	Mesangial matrix score	Podocyte number/glomerulus
db/m CTL	39 ± 4.3	1.49 ± 0.26	11.5 ± 1.5
db/m INO	57 ± 5.5	1.4 ± 0.2	11 ± 0.7
db/db CTL	1,036 ± 180	3.6 ± 0.25	8.05 ± 1.4
db/db INO	440 ± 71*	2.3 ± 0.39*	9.7 ± 0.4*
db/m CTL	14 ± 1	1.2 ± 0.1	10.2 ± 0.4
db/db CTL	721 ± 62	2.9 ± 0.3	7.5 ± 1
db/db PJ-34	397 ± 37*	1.4 ± 0.3*	9.6 ± 1.4*

Data are means ± SE. Albuminuria was measured by murine albumin-specific ELISA kit and creatinine with colorimetric reaction and are expressed as micrograms albumin per milligram creatinine. Mesangial matrix expansion was examined semiquantitatively on PAS-stained kidney sections. Podocyte number per glomerular cross section was counted on frozen sections by WT-1 and synaptopodin double labeling and expressed as mean podocyte number per glomerular cross section. *$P < 0.05$.

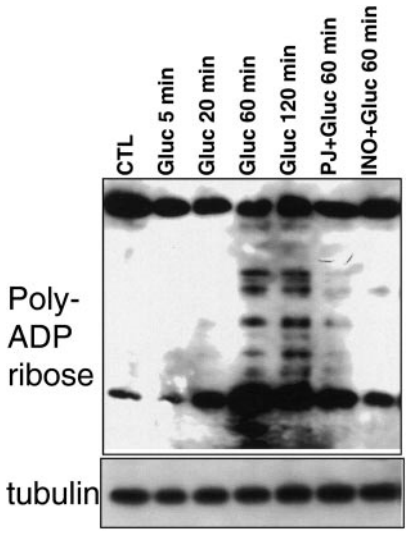

FIG. 3. High glucose leads to an increase of poly(ADP) ribosylated–modified proteins in cultured glomerular epithelial cells. Podocytes were incubated in 5 mmol/l glucose (control [CTL]) or 30 mmol/l glucose (Gluc) for the indicated time periods (5, 20, and 60 min). Cells were pretreated with 3 μmol/l PJ-34 or 200 nmol/l INO-1001, when indicated, followed by incubation with D-glucose. Poly(ADP) ribosylated–modified proteins of whole-cell lysates were detected on Western blot by anti–poly(ADP) ribosylated or αtubulin antibodies.

INO-1001 and PJ-34 inhibit glucose-induced podocyte apoptosis in vitro. We have previously reported that high glucose leads to increased apoptosis of cultured glomerular epithelial cells. Since PARP is an important regulator of apoptosis, we determined the effect of PARP inhibitors INO-1001 or PJ-34 on glucose-induced apoptosis. We observed an increased podocyte apoptosis rate made evident by increased nuclear condensation of cells incubated in a medium containing 30 mmol/l D-glucose (4.2 ± 0.8%) compared with cells incubated in 5 mmol/l D-glucose (1.3 ± 0.2%). Preincubation of cells with 200 nmol/l INO-1001 or 3 μmol/l PJ-34 significantly decreased the degree of glucose-induced apoptosis (Fig. 4*A*). Similarly, both PJ-34 and INO-1001 inhibited hyperglycemia-induced caspase-3 activation (Fig. 4*B*). In summary, PARP inhibitors blocked high-glucose–induced podocyte apoptosis.

PJ-34 and INO-1001 prevent glucose-induced ROS generation in podocytes. PARP has emerged as an important factor in the pathophysiology of reactive species–mediated cell injury. Recent data suggest that PARP could be either a target or an upstream regulator of ROS generation (36,37). Therefore, we next investigated the effect of INO-1001 and PJ-34 on the glucose-induced oxidative stress of glomerular epithelial cells. Incubation of podocytes in high-glucose medium led to an increase of DCF (2′,7′-dichlorofluorescein) fluorescence, which was evident as early as 20 min; however, we observed a slight increase even at earlier time points (Fig. 5*B*). We found that 30 mmol/l D-glucose increased intracellular ROS amount by ~60% (after 4 h incubation) compared with cells incubated in 5 mmol/l glucose with or without 25 mmol/l L-glucose, an osmotic control (Fig. 5*B*). We, similar to other investigators (38), observed an increase in baseline fluorescence of DCF over time, as the dye is light sensitive; however, the glucose-induced increase in fluorescence was fully sensitive to the NADPH oxidase inhibitor dihydrophenyl iodonium (Fig. 5*A*). We found that INO-1001 (200 nmol/l) and PJ-34 (3 μmol/l) treatment abolished glucose-induced intracellular ROS generation of cultured murine podocytes (Fig. 5*A* and *B*).

PJ-34 and INO-1001 prevent mitochondrial depolarization. We next investigated the effect of INO-1001 and PJ-34 on mitochondrial function by determining their effect on mitochondrial membrane potential (32). We found that the incubation of podocytes in 30 mmol/l D-glucose for 4 h caused depolarization of the mitochondria made evident by a shift to the green color of the mitochondrial membrane potential dye JC-1 (Fig. 5*C* and *D*). Preincubation of cells with INO-1001 or PJ-34 prevented mitochondrial membrane depolarization of high-glucose–treated glomerular epithelial cells (Fig. 5*E* and *F*). Quantification of the red and green fluorescence was performed via fluorescence-activated cell sorter analysis on 10,000 JC-1–loaded podocytes. The mean red-to-green fluorescence ratio was 3.6 in control cells, which decreased to 1.2 in cells incubated in 30 mmol/l D-glucose for 18 h, indicating the shift toward the green fluorescence. Preincubation of cells with PJ-34 or INO-1001 prevented the decrease in red fluorescence (Fig. 5*G*), indicating that both inhibitors protect from mitochondrial dysfunction induced by elevated extracellular glucose concentration.

PARP activation inhibits NFκB activation in podocytes. Close association between NFκB and PARP has been described in various cell types (22). We examined

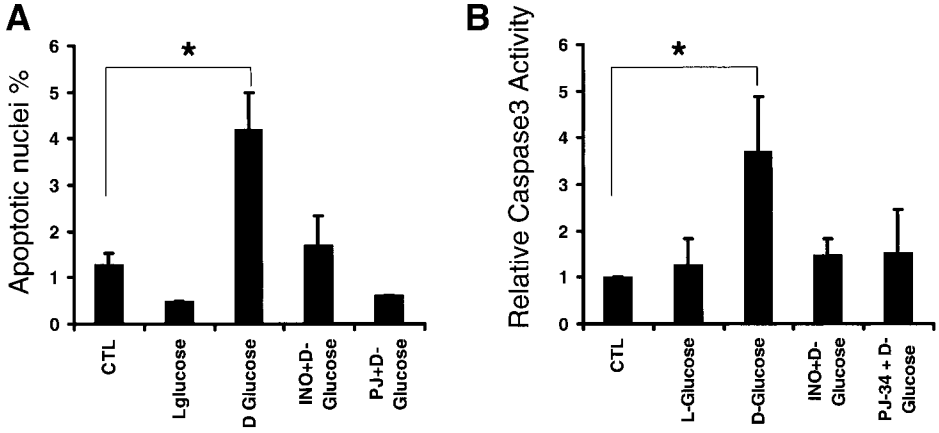

FIG. 4. PARP inhibitors block glucose-induced apoptosis of podocytes. *A*: Nuclear condensation was quantified via DAPI staining after treatment with 200 nmol/l INO-1001 or 3 μmol/l PJ-34 for 45 min, followed by incubation with 30 mmol/l D- or L-glucose for 24 h. *B*: Caspase-3 activity was monitored in 200 nmol/l INO-1001 or 3 μmol/l PJ-34 for 45 min, followed by incubation with 30 mmol/l D- or L-glucose for 18 h. Data are presented as means ± SE of the mean of at least three different experiments. *$P < 0.05$. CTL, control.

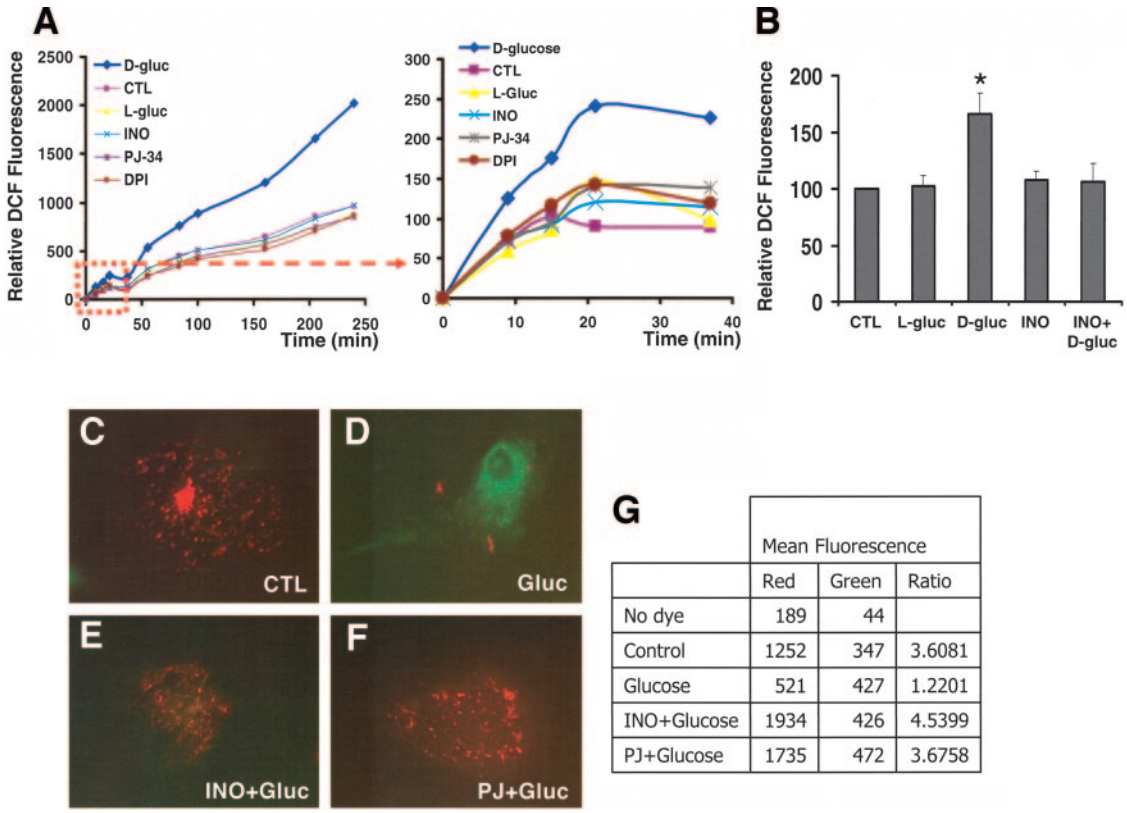

G

	Mean Fluorescence		
	Red	Green	Ratio
No dye	189	44	
Control	1252	347	3.6081
Glucose	521	427	1.2201
INO+Glucose	1934	426	4.5399
PJ+Glucose	1735	472	3.6758

FIG. 5. PARP inhibitors block glucose-induced ROS production and normalize mitochondrial dysfunction in podocytes. *A*: Intracellular ROS release in podocytes was quantified via the changes of DCF fluorescence. Cells were incubated in 5 mmol/l D-glucose or 30 mmol/l D-glucose; 30 mmol/l L-glucose was used as an osmotic control. When indicated, cells were pretreated in 200 nmol/l INO-1001 or 3 μmol/l PJ-34 for 30 min. The *left panel* is a higher magnification of the change of DCF fluorescence during the first 40 min following 30 mmol/l D-glucose treatment. *B*: The percent DCF fluorescence after 4 h treatment in four different experiments. *C–F*: Mitochondrial JC-1 stains of control (*C*) or 30 mmol/l D-glucose (*D*)–treated podocytes. Podocytes were pretreated with INO-1001 (*E*) or PJ-34 (*F*), followed by incubation with 30 mmol/l D-glucose for 4 h. Images are taken with charged-coupled device camera of a fluorescent microscope; images obtained with green and red filters are superimposed. *G*: The mean red and green JC-1 fluorescence (and their ratio) values of 10,000 control and 30 mmol/l D-glucose–treated podocytes in the presence or absence of 200 nmol/l INO-1001 or 3 μmol/l PJ-34 as quantified by fluorescence-activated cell sorter analysis.

whether or not we could observe NFκB activation in vivo in podocytes of diabetic *db/db* mice. We performed immunostaining on kidney sections of control and PJ-34–treated diabetic and nondiabetic samples with NFκB p50 antibody. We found increased nuclear NFκB p50 staining in diabetic *db/db* mice compared with nondiabetic *db/m* mice, indicating an increase of NFκB activity. Double immunostaining with anti-synaptopodin and anti–NFκB p50 showed increased nuclear p50 staining in control *db/db* mice (Fig. 6*A*). Diabetic mice treated with PJ-34 showed less p50 staining compared with control *db/db* mice (Fig. 6*A*).

Next, we determined whether hyperglycemia leads to increased NFκB activation of podocytes in vitro. We detected an increase in the amount of phosphorylated IκBα protein levels in cultured podocytes after 60 min incubation in 30 mmol/l D-glucose (Fig. 6*B*), indicating the activation of the NFκB pathway. Preincubation with PJ-34 or INO-1001 blocked IκBα phosphorylation. In addition, preincubation of cells in apocynin (25 μmol/l), an inhibitor of NADPH oxidase shown to completely block glucose-induced ROS generation (7,38), also prevented the increase in IκBα phosphorylation. Next, we tested the effect of INO-1001 on nuclear translocation NFκB p50 subunit. Nuclear and cytosolic extracts were prepared from podocytes treated with D-glucose for 18 h in the presence or absence of INO-1001. We found increased nuclear NFκB p50 protein expression in cells treated with D-glucose compared with control L-glucose. Similarly, treatment with transforming growth factor-β also resulted in increased nuclear NFκB p50 levels (Fig. 6*C*). Pretreatment with INO-1001 decreased nuclear NFκB p50 levels, likely inhibiting the translocation of this protein in the absence of phosphorylated IκBα. To further confirm the glucose-induced NFκB p50 activation, we performed an ELISA-based NFκB p50 DNA binding assay (Fig. 6*D*). Our data indicate that NFκB is a target of hyperglycemia-induced PARP activation in podocytes.

DISCUSSION

Based on in vivo and in vitro evidence presented in this report, we propose that PARP activation plays an important role in the development of diabetic glomerulopathy in the type 2 diabetes model of Lepr$^{db/db}$ mice. PARP activity is increased in *db/db* mice, which was made evident by an increase in poly(ADP) ribosylated proteins in the kidneys, specifically in glomerular podocytes. Pharmacological inhibition of PARP by two structurally different orally available potent PARP inhibitors (PJ-34 and INO-1001) decreased the development of diabetic glomerular expansion and albuminuria, which are two major hallmarks of diabetic nephropathy.

We propose that prevention of podocyte loss by PARP inhibitors contributes to their observed protective effect. Reports from us and other groups (39–41) indicate that

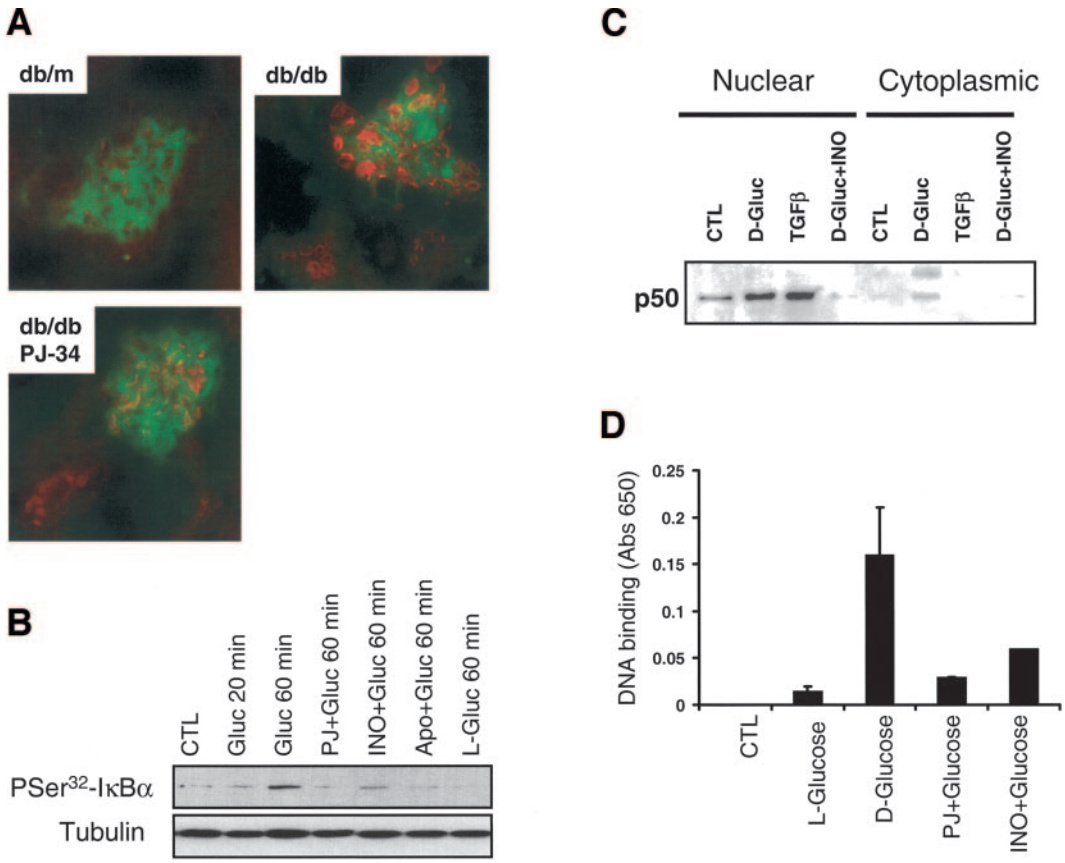

FIG. 6. Role of PARP in NFκB activation of podocytes. *A*: Representative kidney sections of 17-week-old vehicle or PJ-34–treated diabetic *db/db* and control *db/m* mice were stained with NFkB p50 antibody (red) and anti-synapotopodin antibody (green). *B*: Western blot analysis demonstrates levels of phospho-IκBα and tubulin levels in cell lysates of podocytes after treatment with 30 mmol/l D-glucose for 20 and 60 min. When indicated, cells were preincubated with 3 μmol/l PJ-34, 200 nmol/l INO-1001, or 25 μmol/l apocynin (Apo). *C*: Western blot analysis of NFκB p50 levels of protein lysates of conditionally immortalized podocytes after treatment with 30 mmol/l D-glucose, 30 mmol/l L-glucose, and 5 pg/ml transforming growth factor-β (TGFβ) for 18 h. When indicated, cells were pretreated with 200 nmol/l INO-1001 for 30 min before incubation with glucose. *D*: NFκB p50 DNA binding activity was measured in nuclear extracts from podocytes treated in 5 or 30 mmol/l D- or L-glucose for 24 h in the presence or absence of PJ-34 or INO-1001. Data shown are representative results of three independent experiments. CTL, control; Gluc, glucose.

podocyte density plays a central role in the development and progression of diabetic and focal segmental glomerulosclerosis. Podocyte apoptosis and dysfunction can be detected early in the development of diabetic nephropathy, and inhibition of apoptosis was associated with lower albuminuria and less mesangial expansion (7). While we focused our experiments around the dysfunction and apoptosis of glomerular epithelial cells, the effects of PARP inhibitors on other cells types (mesangial and endothelial cells) might also be important in the disease pathogenesis.

PARP inhibitors appear to protect podocytes by multiple mechanisms. First, PJ-34 and INO-1001 prevented high-glucose–induced podocyte apoptosis in vitro. This effect could be related to normalization of the mitochondrial membrane potential, which could protect from mitochondrial collapse. Nuclear translocation of mitochondrial apoptosis–inducing factor, in response to excess PARP-1 activation triggering apoptotic cell death, was found to represent a major cell death pathway in various neuronal and cardiovascular excitotoxicity and oxidative stress models (42–45). NAD^+ depletion and induction of mitochondrial permeability transition were implicated as intermediate steps linking PARP-1 activation to apoptosis-inducing factor translocation. Our results could be consistent with these findings.

PARP inhibitors also blocked high-glucose–induced ROS generation in cultured podocytes. It has long been thought that DNA breaks induced by nitrosative or oxidative stress are the obligatory triggers of PARP activation. Overexpression of uncoupling protein 1 or manganese superoxide dismutase prevents PARP activation in endothelial cells (14). Therefore, PARP activation was placed downstream of intracellular ROS generation. However, here we report that catalytic inhibitors of PARP block high-glucose–induced ROS release. Therefore, it is possible that in high-glucose–treated podocytes, PARP might be activated via an early, and so far unidentified, mechanism and that its activation contributes to an intracellular ROS increase or local ROS generation (not easily assessed by conventional whole-cell ROS assays) that contributes or leads to PARP activation. INO-1001 and PJ-34 are catalytic inhibitors of PARP. (They bind to the active sites.) Therefore, it is unlikely that their ROS inhibitory effect can be attributed to an antioxidant effect, as such an effect is usually observed in much higher concentrations (millimolar). In addition, similar protective results were obtained by other investigators in thymocytes with genetic deletion of PARP-1 and in high-glucose–subjected Schwann cells (36,46).

An additional mechanism that may contribute to the protective effects of PJ-34 and INO-1001 could be re-

lated to the suppression of NFκB activation. Regulation of the NFκB pathway by PARP has been reported in multiple previous studies and has been either attributed to the enzymatic activity of PARP (24) or the physical association of NFκB with PARP (22). In this study, we propose that the catalytic activity of PARP is important in this process. Persistent NFκB activation has been shown in many complication-prone tissues in diabetes, including vascular smooth muscle cells, endothelial cells, pericytes, and renal tubular epithelial cells (47,48). Here, we report that NFκB is activated in high-glucose–treated podocytes in vitro and in podocytes of diabetic mice in vivo. This was made evident by an increase of immunostaining of nuclear NFκB p50 in *db/db* diabetic animals and an increase of IκBα phosphorylation and p50 nuclear translocation following glucose treatment of podocytes. NFκB is a multifunctional transcriptional factor that can regulate the expression of genes involved in cell survival, apoptosis, and inflammatory response. Recent reports indicate that NFκB might play an important role in the pathogenesis of diabetic nephropathy of streptozotocin-induced diabetic rats (48), although the exact mechanism of activation and its downstream effectors are not fully established. In the case of HIV-infected podocytes, Fas and FasL was shown to be directly regulated by NFκB (49). We have also observed an increase of FasL mRNA in high-glucose–treated podocytes (K.S., unpublished observations). Since FasL plays an important role in the apoptosis pathway, it might also represent a link by which PARP inhibitors protect podocytes from high-glucose–induced apoptosis. However, other effects of NFκB should not be excluded.

In summary, we propose that PARP activation plays an important role in the development of diabetic glomerulopathy, as inhibitors of this enzyme attenuate the development of glomerular changes in Lepr$^{db/db}$ mice, a model of type 2 diabetes. We propose that PARP activation is an important central mediator of hyperglycemia-induced podocyte dysfunction. PARP inhibitors block high-glucose–induced podocyte apoptosis, ROS generation, and the activation of the NFκB pathway and can subsequently protect from podocyte loss. This conclusion may be particularly significant, as PARP inhibitors are currently in clinical trials for various other indications (15). Based on our findings, we suggest that they may also be beneficial in diabetic nephropathy.

ACKNOWLEDGMENTS

This work was supported by grants from the Juvenile Diabetes Foundation, the National Kidney Foundation, the National Institutes of Health, the Hungarian Research Fund OTKA, and the European Foundation for the Study of Diabetes.

Cell culture and histology service were provided by the O'Brian Kidney Center Imaging Core Facility.

We thank Mr. Chih-Kang Huang and Chun-Yang Xiao for their technical assistance with the animal experiments. We also thank Dr. Peter Mundel (Mount Sinai School of Medicine) for providing the murine podocyte cell line and Dr. Thomas Hostetter for a critical reading of the manuscript.

REFERENCES

1. Centers for Disease Control and Prevention: State-specific trends in chronic kidney failure: United States, 1990–2001. *MMWR Morb Mortal Wkly Rep* 53:918–920, 2004
2. Fioretto P, Steffes MW, Brown DM, Mauer SM: An overview of renal pathology in insulin-dependent diabetes mellitus in relationship to altered glomerular hemodynamics. *Am J Kidney Dis* 20:549–558, 1992
3. Retinopathy and nephropathy in patients with type 1 diabetes four years after a trial of intensive therapy: the Diabetes Control and Complications Trial/Epidemiology of Diabetes Interventions and Complications Research Group. *N Engl J Med* 342:381–389, 2000
4. Danesh FR, Kanwar YS: Modulatory effects of HMG-CoA reductase inhibitors in diabetic microangiopathy. *FASEB J* 18:805–815, 2004
5. Ziyadeh FN, Sharma K: Overview: combating diabetic nephropathy. *J Am Soc Nephrol* 14:1355–1357, 2003
6. Wolf G, Chen S, Ziyadeh FN: From the periphery of the glomerular capillary wall toward the center of disease: podocyte injury comes of age in diabetic nephropathy. *Diabetes* 54:1626–1634, 2005
7. Susztak K, Raff AC, Schiffer M, Bottinger EP: Glucose-induced reactive oxygen species cause apoptosis of podocytes and podocyte depletion at the onset of diabetic nephropathy. *Diabetes* 55:225–233, 2006
8. Kriz W, Gretz N, Lemley KV: Progression of glomerular diseases: is the podocyte the culprit? *Kidney Int* 54:687–697, 1998
9. Pavenstadt H, Kriz W, Kretzler M: Cell biology of the glomerular podocyte. *Physiol Rev* 83:253–307, 2003
10. Meyer TW, Bennett PH, Nelson RG: Podocyte number predicts long-term urinary albumin excretion in Pima Indians with type II diabetes and microalbuminuria. *Diabetologia* 42:1341–1344, 1999
11. Petermann AT, Pippin J, Krofft R, Blonski M, Griffin S, Durvasula R, Shankland SJ: Viable podocytes detach in experimental diabetic nephropathy: potential mechanism underlying glomerulosclerosis. *Nephron Exp Nephrol* 98:e114–e123, 2004
12. Asaba K, Tojo A, Onozato ML, Goto A, Quinn MT, Fujita T, Wilcox CS: Effects of NADPH oxidase inhibitor in diabetic nephropathy. *Kidney Int* 67:1890–1898, 2005
13. Brownlee M: Biochemistry and molecular cell biology of diabetic complications. *Nature* 414:813–820, 2001
14. Du X, Matsumura T, Edelstein D, Rossetti L, Zsengeller Z, Szabo C, Brownlee M: Inhibition of GAPDH activity by poly(ADP-ribose) polymerase activates three major pathways of hyperglycemic damage in endothelial cells. *J Clin Invest* 112:1049–1057, 2003
15. Jagtap P, Szabo C: Poly(ADP-ribose) polymerase and the therapeutic effects of its inhibitors. *Nat Rev Drug Discov* 4:421–440, 2005
16. Pacher P, Szabo C: Role of poly(ADP-ribose) polymerase-1 activation in the pathogenesis of diabetic complications: endothelial dysfunction, as a common underlying theme. *Antioxid Redox Signal* 7:1568–1580, 2005
17. Jagtap PG, Baloglu E, Southan GJ, Mabley JG, Li H, Zhou J, van Duzer J, Salzman AL, Szabo C: Discovery of potent poly(ADP-ribose) polymerase-1 inhibitors from the modification of indeno[1,2-c]isoquinolinone. *J Med Chem* 48:5100–5103, 2005
18. Li F, Drel VR, Szabo C, Stevens MJ, Obrosova IG: Low-dose poly(ADP-ribose) polymerase inhibitor-containing combination therapies reverse early peripheral diabetic neuropathy. *Diabetes* 54:1514–1522, 2005
19. Farivar AS, McCourtie AS, MacKinnon-Patterson BC, Woolley SM, Barnes AD, Chen M, Jagtap P, Szabo C, Salerno CT, Mulligan MS: Poly (ADP) ribose polymerase inhibition improves rat cardiac allograft survival. *Ann Thorac Surg* 80:950–956, 2005
20. Szabo C: Poly(ADP-ribose) polymerase activation by reactive nitrogen species: relevance for the pathogenesis of inflammation. *Nitric Oxide* 14:169–179, 2006
21. Pieper AA, Brat DJ, Krug DK, Watkins CC, Gupta A, Blackshaw S, Verma A, Wang ZQ, Snyder SH: Poly(ADP-ribose) polymerase-deficient mice are protected from streptozotocin-induced diabetes. *Proc Natl Acad Sci U S A* 96:3059–3064, 1999
22. Zheng L, Szabo C, Kern TS: Poly(ADP-ribose) polymerase is involved in the development of diabetic retinopathy via regulation of nuclear factor-κB. *Diabetes* 53:2960–2967, 2004
23. Obrosova IG, Li F, Abatan OI, Forsell MA, Komjati K, Pacher P, Szabo C, Stevens MJ: Role of poly(ADP-ribose) polymerase activation in diabetic neuropathy. *Diabetes* 53:711–720, 2004
24. Garcia Soriano F, Virag L, Jagtap P, Szabo E, Mabley JG, Liaudet L, Marton A, Hoyt DG, Murthy KG, Salzman AL, Southan GJ, Szabo C: Diabetic endothelial dysfunction: the role of poly(ADP-ribose) polymerase activation. *Nat Med* 7:108–113, 2001
25. Szabo C: PARP as a drug target for the therapy of diabetic cardiovascular dysfunction. *Drug News Perspect* 15:197–205, 2002

26. Minchenko AG, Stevens MJ, White L, Abatan OI, Komjati K, Pacher P, Szabo C, Obrosova IG: Diabetes-induced overexpression of endothelin-1 and endothelin receptors in the rat renal cortex is mediated via poly(ADP-ribose) polymerase activation. *FASEB J* 17:1514–1516, 2003
27. Breyer MD, Bottinger E, Brosius FC 3rd, Coffman TM, Harris RC, Heilig CW, Sharma K: Mouse models of diabetic nephropathy. *J Am Soc Nephrol* 16:27–45, 2005
28. Susztak K, Ciccone E, McCue P, Sharma K, Bottinger EP: Multiple metabolic hits converge on CD36 as novel mediator of tubular epithelial apoptosis in diabetic nephropathy. *PLoS Med* 2:e45, 2005
29. Szabo C, Zanchi A, Komjati K, Pacher P, Krolewski AS, Quist WC, LoGerfo FW, Horton ES, Veves A: Poly(ADP-ribose) polymerase is activated in subjects at risk of developing type 2 diabetes and is associated with impaired vascular reactivity. *Circulation* 106:2680–2686, 2002
30. Schiffer M, Mundel P, Shaw AS, Bottinger EP: A novel role for the adaptor molecule CD2-associated protein in transforming growth factor-beta-induced apoptosis. *J Biol Chem* 279:37004–37012, 2004
31. Mundel P, Heid HW, Mundel TM, Kruger M, Reiser J, Kriz W: Synaptopodin: an actin-associated protein in telencephalic dendrites and renal podocytes. *J Cell Biol* 139:193–204, 1997
32. Konrad D, Rudich A, Bilan PJ, Patel N, Richardson C, Witters LA, Klip A: Troglitazone causes acute mitochondrial membrane depolarisation and an AMPK-mediated increase in glucose phosphorylation in muscle cells. *Diabetologia* 48:954–966, 2005
33. Ziyadeh FN, Hoffman BB, Han DC, Iglesias-De La Cruz MC, Hong SW, Isono M, Chen S, McGowan TA, Sharma K: Long-term prevention of renal insufficiency, excess matrix gene expression, and glomerular mesangial matrix expansion by treatment with monoclonal antitransforming growth factor-beta antibody in db/db diabetic mice. *Proc Natl Acad Sci U S A* 97:8015–8020, 2000
34. Susztak K, Bottinger E, Novetsky A, Liang D, Zhu Y, Ciccone E, Wu D, Dunn S, McCue P, Sharma K: Molecular profiling of diabetic mouse kidney reveals novel genes linked to glomerular disease. *Diabetes* 53:784–794, 2004
35. Steinke JM, Sinaiko AR, Kramer MS, Suissa S, Chavers BM, Mauer M: The early natural history of nephropathy in type 1 diabetes. III. Predictors of 5-year urinary albumin excretion rate patterns in initially normoalbuminuric patients. *Diabetes* 54:2164–2171, 2005
36. Obrosova IG, Drel VR, Pacher P, Ilnytska O, Wang ZQ, Stevens MJ, Yorek MA: Oxidative-nitrosative stress and poly(ADP-ribose) polymerase (PARP) activation in experimental diabetic neuropathy: the relation is revisited. *Diabetes* 54:3435–3441, 2005
37. Virag L, Szabo C: Purines inhibit poly(ADP-ribose) polymerase activation and modulate oxidant-induced cell death. *FASEB J* 15:99–107, 2001
38. Kim NH, Rincon-Choles H, Bhandari B, Choudhury GG, Abboud HE, Gorin Y: Redox dependence of glomerular epithelial cell hypertrophy in response to glucose. *Am J Physiol Renal Physiol* 290:F741–F751, 2006
39. Wiggins JE, Goyal M, Sanden SK, Wharram BL, Shedden KA, Misek DE, Kuick RD, Wiggins RC: Podocyte hypertrophy, "adaptation," and "decompensation" associated with glomerular enlargement and glomerulosclerosis in the aging rat: prevention by calorie restriction. *J Am Soc Nephrol* 16:2953–2966, 2005
40. Wharram BL, Goyal M, Wiggins JE, Sanden SK, Hussain S, Filipiak WE, Saunders TL, Dysko RC, Kohno K, Holzman LB, Wiggins RC: Podocyte depletion causes glomerulosclerosis: diphtheria toxin-induced podocyte depletion in rats expressing human diphtheria toxin receptor transgene. *J Am Soc Nephrol* 16:2941–2952, 2005
41. Schiffer M, Bitzer M, Roberts IS, Kopp JB, ten Dijke P, Mundel P, Bottinger EP: Apoptosis in podocytes induced by TGF-beta and Smad7. *J Clin Invest* 108:807–816, 2001
42. Chen M, Zsengeller Z, Xiao CY, Szabo C: Mitochondrial-to-nuclear translocation of apoptosis-inducing factor in cardiac myocytes during oxidant stress: potential role of poly(ADP-ribose) polymerase-1. *Cardiovasc Res* 63:682–688, 2004
43. Xiao CY, Chen M, Zsengeller Z, Li H, Kiss L, Kollai M, Szabo C: Poly(ADP-ribose) polymerase promotes cardiac remodeling, contractile failure, and translocation of apoptosis-inducing factor in a murine experimental model of aortic banding and heart failure. *J Pharmacol Exp Ther* 312:891–898, 2005
44. Yu SW, Wang H, Poitras MF, Coombs C, Bowers WJ, Federoff HJ, Poirier GG, Dawson TM, Dawson VL: Mediation of poly(ADP-ribose) polymerase-1-dependent cell death by apoptosis-inducing factor. *Science* 297:259–263, 2002
45. Dawson VL, Dawson TM: Deadly conversations: nuclear-mitochondrial cross-talk. *J Bioenerg Biomembr* 36:287–294, 2004
46. Virag L, Salzman AL, Szabo C: Poly(ADP-ribose) synthetase activation mediates mitochondrial injury during oxidant-induced cell death. *J Immunol* 161:3753–3759, 1998
47. Morcos M, Sayed AA, Bierhaus A, Yard B, Waldherr R, Merz W, Kloeting I, Schleicher E, Mentz S, Abd el Baki RF, Tritschler H, Kasper M, Schwenger V, Hamann A, Dugi KA, Schmidt AM, Stern D, Ziegler R, Haering HU, Andrassy M, van der Woude F, Nawroth PP: Activation of tubular epithelial cells in diabetic nephropathy. *Diabetes* 51:3532–3544, 2002
48. Lee FT, Cao Z, Long DM, Panagiotopoulos S, Jerums G, Cooper ME, Forbes JM: Interactions between angiotensin II and NF-kappaB-dependent pathways in modulating macrophage infiltration in experimental diabetic nephropathy. *J Am Soc Nephrol* 15:2139–2151, 2004
49. Ross MJ, Martinka S, D'Agati VD, Bruggeman LA: NF-kappaB regulates Fas-mediated apoptosis in HIV-associated nephropathy. *J Am Soc Nephrol* 16:2403–2411, 2005